Wavelet Analysis in Infantile Nystagmus Syndrome: Limitations and Abilities

Larry A. Abel,[1] Zhong I. Wang,[2,3] and Louis F. Dell'Osso[2,3,4]

PURPOSE. To investigate the proper usage of wavelet analysis in infantile nystagmus syndrome (INS) and determine its limitations and abilities.

METHODS. Data were analyzed from accurate eye-movement recordings of INS patients. Wavelet analysis was performed to examine the foveation characteristics, morphologic characteristics and time variation in different INS waveforms. Also compared were the wavelet analysis and the expanded nystagmus acuity function (NAFX) analysis on sections of pre- and post-tenotomy data.

RESULTS. Wavelet spectra showed some sensitivity to different features of INS waveforms and reflected their variations across time. However, wavelet analysis was not effective in detecting foveation periods, especially in a complicated INS waveform. NAFX, on the other hand, was a much more direct way of evaluating waveform changes after nystagmus treatments.

CONCLUSIONS. Wavelet analysis is a tool that performs, with difficulty, some things that can be done faster and better by directly operating on the nystagmus waveform itself. It appears, however, to be insensitive to the subtle but visually important improvements brought about by INS therapies. Wavelet analysis may have a role in developing automated waveform classifiers where its time-dependent characterization of the waveform can be used. The limitations of wavelet analysis outweighed its abilities in INS waveform-characteristic examination. (*Invest Ophthalmol Vis Sci.* 2008;49:3413–3423) DOI:10.1167/iovs.08-1710

The oscillatory nature of infantile nystagmus syndrome (INS)[1] has prompted researchers to use advanced mathematical tools such as spectral analysis and wavelet analysis for the purpose of understanding the etiology of this disorder. INS is not a stationary process. The waveforms of INS may become worse with gaze position or during stress or visual demand.[2-5] Conversely, loss of attention to an object being viewed may lead to the nystagmus' diminishing. For this reason, studies of nystagmus generally analyze data segments lasting only 5 to 10 seconds.

A further problem arises when trying to characterize INS with signal processing techniques, even if applied over intervals of only several seconds. The most crucial feature of the waveform in terms of its effect on visual acuity is the amount of time in each cycle of the oscillation during which the retinal image of the object of regard is on or near the fovea and either stationary or moving relatively slowly. It has repeatedly been shown that longer durations of these *foveation periods* facilitate better acuity.[2,6-11] These key features of the INS waveform have durations measured in tens of milliseconds. Identifying features at this time scale is beyond the resolution of even the short-time Fourier transform (STFT, see the Discussion section). Foveation characteristics have historically been examined by differentiating the INS position signal and identifying those periods in the waveform that meet specific position and velocity criteria.[2,12-19] These criteria have been incorporated into the expanded nystagmus acuity function (NAFX),[9,20,21] which may be used to predict the best potential visual acuity possible for a given waveform in the absence of a visuosensory abnormality.

Ideally, one would like to be able to analyze nystagmus waveforms by using a technique that could provide a global representation of the waveform in the way that a Fourier spectrum does, but that also can localize in time the specific features of the waveform such as the foveation periods. One attractive candidate for this is the wavelet transform. Unlike STFT, wavelet analysis uses a suite of scaled basis functions derived from a "mother wavelet." The signal being analyzed is represented by coefficients, roughly analogous to the amplitude spectrum derived via Fourier analysis. However, these coefficients are not constants but instead vary continuously across time. They represent the relative weighting at each instant of wavelets with scales varying from the rapidly to the slowly changing, again analogous to how conventional spectral analysis displays the frequency components of a signal. The key difference, however, is that the wavelet coefficients, being functions of time, allow the user to see how this "spectral" representation changes moment by moment. For instance, this allows wavelet analysis to localize a brief transient intrusion into a periodic waveform, whereas it would be essentially undetectable in conventional spectral analysis because the transient would contribute little to the overall energy of the signal. Wavelet analysis has been used to separate fast and slow phases in caloric nystagmus,[22] to detect features in the electrocardiogram (ECG),[23] and to identify the time of muscle contraction in surface electromyograms (EMGs),[24] among other physiological applications. It has also been used to identify seizure activity and other features of the electroencephalogram (EEG).[25,26]

As noted previously, in INS the functional part of the waveform (i.e., the foveation periods[27,28]) is small compared with the nonfunctional parts outside of the foveation window. Although wavelet analysis is well-suited to identifying time-varying changes in a waveform, it is not at all clear that, when applied to an INS eye movement recording, it would offer any advantage over the more direct application of velocity and position criteria for foveation, which have been used for many years. INS has been examined using this approach only once

before, by Miura et al.[29,30] However, they averaged the wavelet coefficients obtained over the entire several-minutes' duration of the recordings. Although wavelet analysis may be useful in identifying some time-associated changes in nystagmus, it is not obvious how such a "global" parameter calculation can be used to detect the foveation parts of the waveforms.

The purpose of this study was to investigate whether wavelet analysis, used appropriately, can detect the foveation periods (the only functionally important part of the waveform contributing to visual acuity), foveation changes in INS resulting from tenotomy, morphology of different INS waveforms (pendular, jerk, pendular with foveating saccade [Pfs], pseudopendular with foveating saccades [PPfs], and dual jerk [DJ]), waveform time variation, and inattention. We thus examined the wavelet coefficient amplitudes and contour plots across each record.

Finding the most sensitive analysis method for INS waveforms is important for the development of objective methods of evaluating the success of therapeutic procedures on patients with INS. The four-muscle tenotomy procedure was based on the secondary null broadening effects of the Kestenbaum procedure[31-33] first described in 1979.[34-36] This surgery for nystagmus consists of detaching the muscle at the insertion end of the tendon and reattaching it at the same place with absorbable sutures. Tenotomy effectively decreases the gain of the ocular motor plant to small, nonsaccadic signals[37] and elevates foveation quality. It has been shown to be efficacious for INS, acquired nystagmus (pendular and jerk, horizontal and vertical) and to reduce the associated oscillopsia.[4,10,20,21,38-41] Since the tenotomy procedure improves the foveation periods, not necessarily the intensity of the nystagmus, it is crucial to examine only the foveation periods for the surgical effects, rather than the nystagmus intensity or the spectral average holistically calculated.

In this study, we examined the following: (1) concatenated short records (5–10 seconds of data) with steady fixation; (2) pre- and post-tenotomy fixation data; (3) long fixation records of several minutes of asymmetric (a)periodic alternating nystagmus (APAN); (4) inattention and DJ data containing several frequency components.

METHODS

Recording

Infrared reflection and high-speed digital video were used for the eye-movement recording. The infrared reflection system (Applied Scientific Laboratories, Waltham, MA) was linear to 20° in the horizontal plane and monotonic to 25° to 30° with a sensitivity of 0.25°. The total system bandwidth (position and velocity) was 0 to 100 Hz. The data were digitized at 500 Hz with 16-bit resolution. The digital video system (EyeLink II; SR Research, Mississauga, ON, Canada) had a linear range of ±30° horizontally and ±20° vertically. The system's sampling frequency was 500 Hz, and the gaze position accuracy error was 0.5° to 1° on average. The data were digitized at 500 Hz with 16-bit resolution. The infrared reflection (Eyelink signal) from each eye was calibrated with the other eye covered to obtain accurate position information; the foveation periods were used for calibration. The accurate position data of each eye allows determination of both the smallest amount of strabismus throughout the trial and the fixating eye. Only the fixating-eye data were analyzed, as the other eye makes no contribution to visual acuity.

Protocol

This study was approved by the local institutional review board. Written consent was obtained from subjects before the testing, in accordance with the Declaration of Helsinki. All test procedures were carefully explained to each subject before the experiment began, and

were reinforced with verbal commands during the trials. The subjects were seated in a chair with headrest and a chin stabilizer, far enough (>5 feet) from the red reflected laser target to prevent convergence effects. At this distance, the reflected laser target subtended less than 0.1° of visual angle. The room light remained blacked out throughout the recordings. An experiment consisted of from 8 to 10 trials, each lasting under 2 minutes with time allowed between trials for the subject to rest. Trials were kept this short to guard against boredom, because IN intensity is known to decrease with inattention. Subjects were instructed to look at the target with the head in primary position.
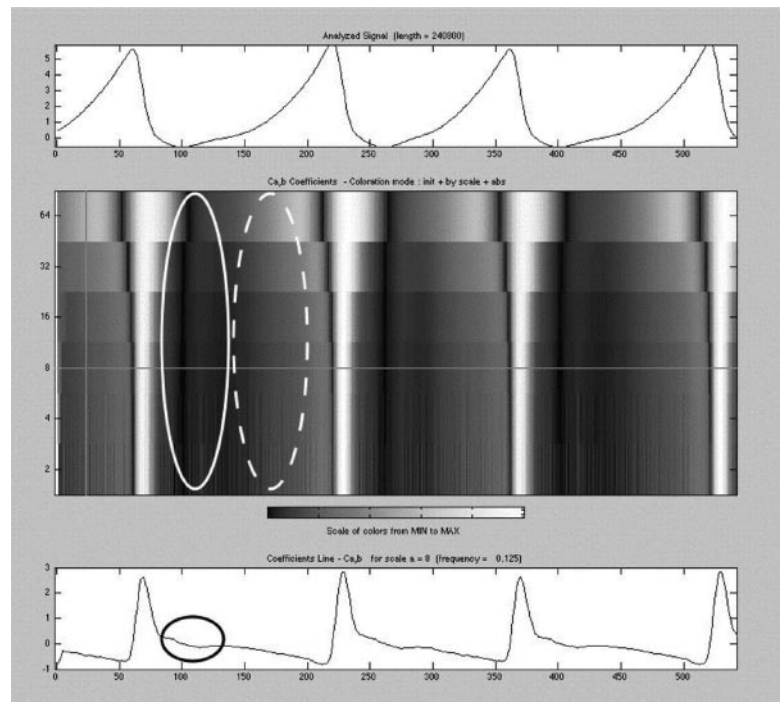
Analysis

A wavelet is a mathematical function that divides a given function into different frequency components to study each component with a resolution that matches its scale. Unlike Fourier analysis, in which signals are analyzed using sine and cosine waves, a wavelet transform is the representation of a function by basis functions that are scaled and translated copies (the "daughter wavelets") of a finite-length or fast-decaying oscillating waveform (the "mother wavelet"). Wavelet transforms have advantages over Fourier transforms for representing functions that are nonstationary, especially those that have discontinuities and sharp peaks. We used commercial software (Wavelet Toolbox in MatLab; The MathWorks, Natick, MA) for the analysis. We chose the Haar harmonics in continuous wavelet analysis, and power-2 mode or step-by-step mode. The maximum number of the steps varied, as will be specified in the Results section. The Haar wavelet is the oldest and simplest wavelet in use.[42] It is computationally efficient and, after empiric testing, was better than alternative wavelets at generating coefficients that, on some scales, resembled familiar functions such as eye velocity. Use of the power-2 mode offered computational advantages over the step-by-step mode that were analogous to those the fast Fourier transform offers over the continuous Fourier transform. The use of a power of 6 was determined empirically, when adding additional levels yielded coefficients containing mostly noise. We have also included several of the computationally more intensive step-by-step examples (see Figs. 6, 9, 10) to show the nature of the more continuous contour plots. However, a given coefficient line for the same data is the same when computed using either approach.

As pointed out in the introduction, steady fixation for long periods is difficult to obtain in patients with INS. Even in normal subjects, boredom and blinking frequently occur. We used shorter periods of good fixation (<10 seconds) and concatenated them to produce long data records (~8 minutes) of "good fixation." We also included in the analysis long, nonconcatenated records containing periods of fixating-eye switches, failure to maintain fixation, and inattention. These records were analyzed to determine whether wavelets could detect the differences between the records of good fixation and those containing interruptions of good fixation that decrease visual acuity.

The NAFX[9] was used to demonstrate the difference in a pre- and a postsurgical fixation segment from one patient. The NAFX is an objective measure of waveform foveation quality. It predicts potential visual acuity in nystagmus patients, assuming no sensory deficits. It is a direct measurement of the eye-movement effects of nystagmus therapies. It could be applied to any nystagmus waveform with a position and velocity variability lying within the maximum foveation window of ±6 and ±10°/s. All the NAFX analysis was performed in the MatLab environment using OMLAB (Ocular Motility Laboratory) software (OMtools, downloadable from http://www.omlab.org, provided in the public domain by the The Daroff-Dell'Osso Ocular Motility Laboratory, Louis Stokes Cleveland Department of Veterans Affairs Medical Center, Case School of Medicine, Case Western Reserve University, Cleveland, OH). Details of how to perform NAFX analysis properly can be found on http://www.omlab.org/OMLAB_page/Teaching/Using_NAFX.html.

FIGURE 1. One-dimensional continuous wavelet transform of a jerk left waveform with mediocre foveation (power 6 in power-2 mode). *Solid white ellipse*: the foveation after the saccade in one cycle; *dashed white ellipse*: slow-phase runaway; *solid black ellipse*: the coefficient line at 8 indicates a flat foveation period. In this and the remaining figures: *top trace*: the waveform; *middle contours*: grayscale-coded plots of the absolute values of the wavelet coefficients; *bottom trace:* the wavelet output at a certain coefficient without taking the absolute value. The *y*-axes in the contour plots roughly correspond to the inverse of frequency. The *x*-axes are in milliseconds.

RESULTS

Wavelet Analysis of the Foveation Characteristics of INS Waveforms

Figure 1 shows the wavelet analysis result of a jerk left waveform with mediocre foveation. The top trace in the panel is the waveform (a zoomed-in section of the 8-minute concatenated data); the middle contours are color-coded plots of the absolute values of the wavelet coefficients generated using the Haar wavelet (power-2 mode, power level 6). The *y*-axis roughly corresponds to the inverse of frequency (i.e., the small numbers [scales] represent the equivalent of high frequencies). Unless otherwise stated, we used power level 6 in power-2 mode. Power 6 was chosen because higher levels did not show much additional information in these particular cases. Absolute-value mode for the contour plot was used because it made the foveation periods in the contour plot more evident. The bottom trace is the wavelet output at a certain selected coefficient (designated by the position of the horizontal cursor crossing the contour plot) without taking the absolute value.

In Figure 1, the foveation after the saccade in each cycle corresponds to a darker, low-energy area (shown in the solid white ellipse), followed by a lighter area corresponding to the slow-phase runaway (shown in the dashed white ellipse). The coefficient line at 8 clearly indicates the flat foveation period, shown in the black ellipse. The wavelet analysis at this coefficient acted like a differentiator, clearly showing the saccades. This coefficient line was chosen because it offered good distinction between the foveation and the slow phase and contained little high-frequency noise. The wavelet analysis toolbox offers the ability to choose the level of "differentiation" to best indicate foveation.

Figure 2 demonstrates a jerk right waveform with good foveation in each cycle (for ease of comparison, Figs. 1, 2 have approximately the same data length). Compared with Figure 1, the darker area (solid white ellipse) after the saccade (white spike) covered much more percentage space in each cycle. Again the dashed white ellipse shows the slow phase, and the black ellipse shows the foveation period on the level-8 coefficient line.

In comparing Figures 1 and 2, by identifying the darker areas after the foveating saccade, the foveation quality can be visualized. Both the contour plot and the coefficient line can contribute to this identification. As the waveforms get more complicated, however, the identification process may be less obvious. In Figure 3, we show an example of a PPfs waveform. In this case, there are two saccades per cycle. The solid white ellipse shows the real foveation period in the contour plot, followed by the slow-phase runaway (dashed white ellipse). A second saccade (the braking saccade) follows (dotted white ellipse), the area after which could be confused with foveation. The braking saccade is again followed by a slow-phase runaway, shown in the dashed black ellipse. Since there is not much cessation of movement (and no true foveation) after the braking saccade, the area in the contour plot is not as dark (compare the dotted white ellipse with the solid white one).

Wavelet Analysis of Pre- and Post-tenotomy Data

Figure 4a is a section of fixation from a patient with INS pre-tenotomy. This segment has a mixture of pendular and Pfs waveforms, and the foveation was not well developed. From the wavelet analysis output, one cannot define the foveation periods as clearly as in Figures 1, 2, and 3. The NAFX output for the same segment is shown in Figures 4b and 4c, with an NAFX output = 0.121 (VA ≈ 20/195+) in this 15-year-old patient.

We performed a post-tenotomy wavelet analysis of the data from the same patient (Fig. 5a). A comparison of Figures 4 and 5 shows that there are differences in the size of the darker area after foveating saccades. In this case, the waveforms are more complicated than pure jerk or pendular waveforms, and so the foveation is less clearly shown compared with previous examples. The NAFX for the same segment is 0.343 (VA ≈ 20/50+); that is, a ~180% increase from the pre-tenotomy NAFX of 0.121. Output of the NAFX calculation is shown in Figures 5b and 5c.

Wavelet Analysis of the Morphologic Characteristics of INS Waveforms

Figure 6 shows a subject with APAN. We chose the step-by-step mode with a maximum number of 512 steps in this example.
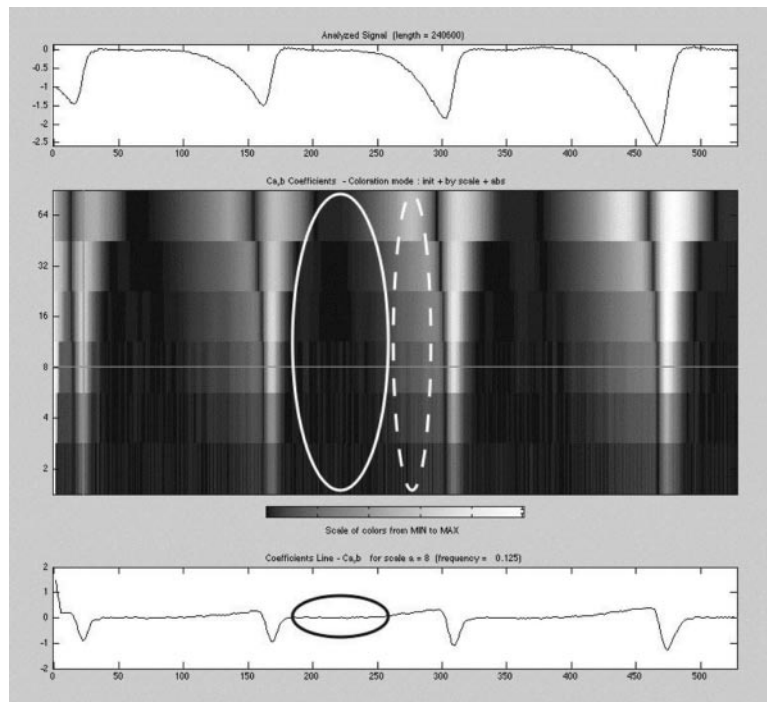
FIGURE 2. One-dimensional continuous wavelet transform of a jerk right waveform with good foveation (power 6 in power-2 mode). The ellipses are as described in Figure 1. The *x*-axes are in milliseconds.

The bottom trace demonstrates the high-frequency pendular component that is sampled with a low wavelet coefficient (the cursor on the contour plot was set near the bottom and therefore is difficult to see). The pendular component was always present in the waveform, despite direction changes and can be seen most prominently in the coefficient contour plot at the low scales (e.g., at the cursor position), which correspond to higher frequencies. The fast-phase direction change also shows well. The solid ellipse identifies the left-beating components, the dashed ellipse, the right-beating. In the contour plot, the saccades in the DJ waveform at the beginning and end of the segment were characterized by spiky patterns, whereas the middle transitional pendular part showed a more homogeneous pattern. A blink at about $t = 1750$ seconds is prominent throughout the plot, reflecting the wavelet transform's ability to localize transient events temporally.

In the inattention data piece in Figure 7, the saccade that brought the wandering eye back to the target is clearly shown as a white, high-energy spike. The dashed white ellipse shows a different pattern than does the solid white, because no saccades were made during this inattention period, and therefore, no effective foveation was produced.
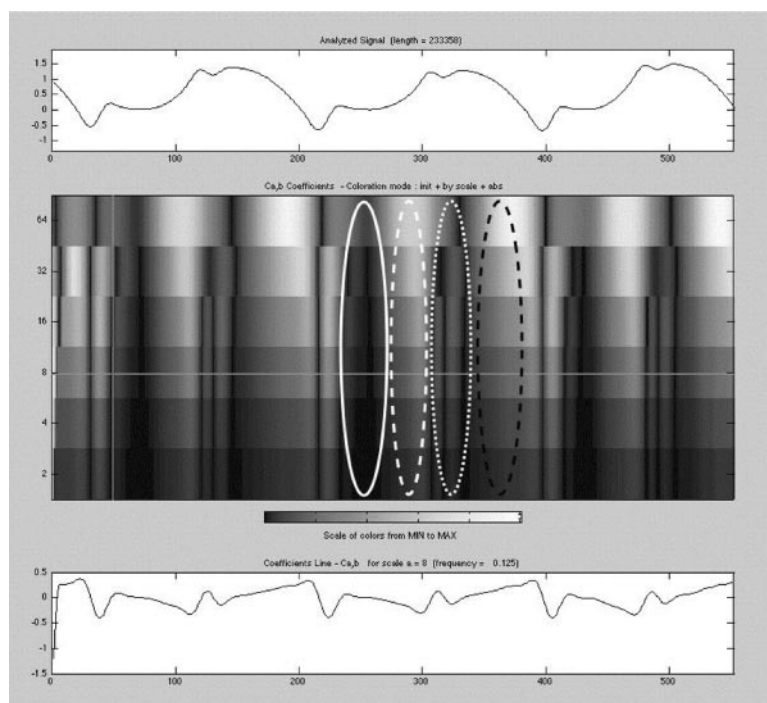

FIGURE 3. One-dimensional continuous wavelet transform of a PPfs waveform (power 6 in power-2 mode). *Solid white ellipse*: real foveation period in the contour plot; *dashed white ellipse*: slow-phase runaway; *dotted white ellipse*: a second saccade (the braking saccade); *dashed black ellipse*: braking saccade is followed by another slow-phase runaway. The *x*-axes are in milliseconds.
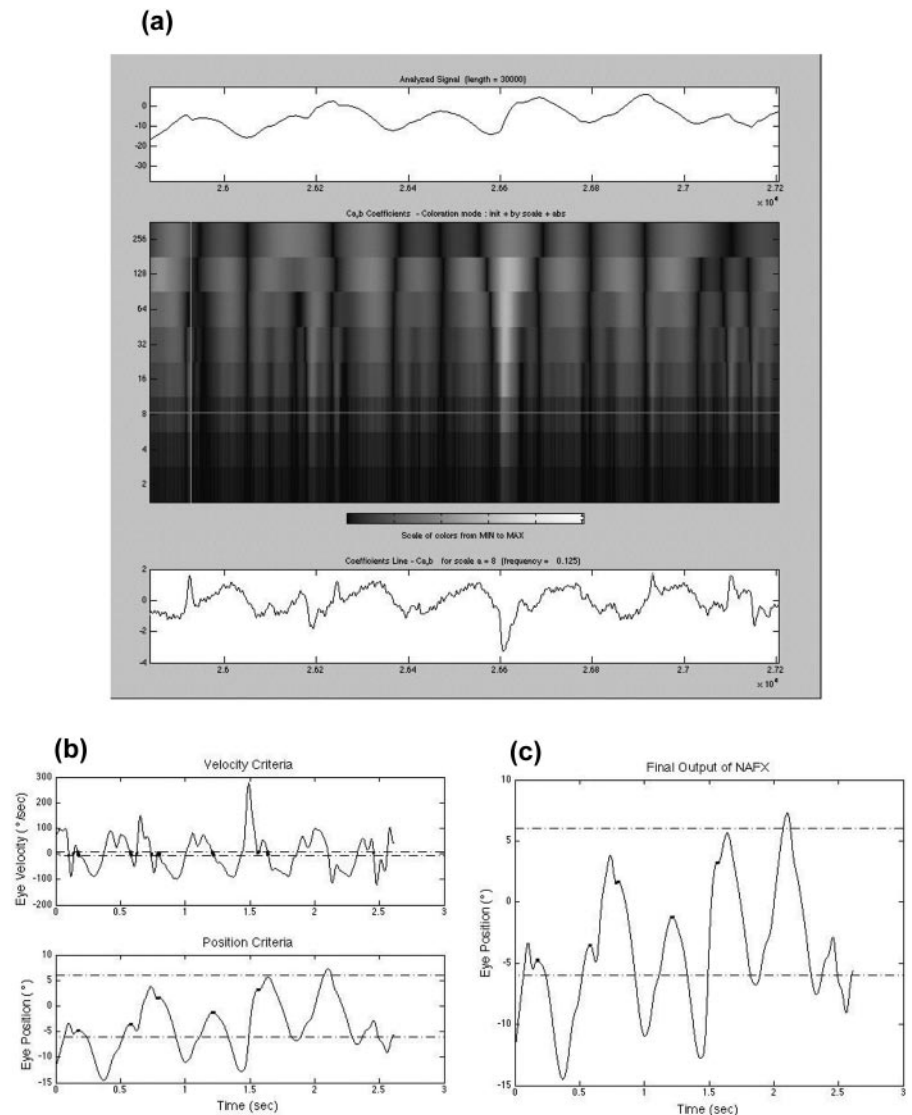
FIGURE 4. (a) One-dimensional continuous wavelet transform of pretenotomy fixation data from a 15-year-old patient (power 6 in power-2 mode). The coefficient line at 8 was shown as the bottom trace. (b) NAFX analysis of the same data section. *Bold dots*: the part in the waveform meeting the velocity (*top*) and position (lower panel) requirement. (c) Output of the NAFX analysis combining the two requirements in (b). The integrated output corresponds to an NAFX value of 0.121. The *x*-axes are in seconds.

Again we see the darker areas after each foveating saccade in the solid white ellipse region. Although there are also darker stripes within the dashed white ellipse, they cannot be counted as foveating periods, because there are no preceding foveating saccades.

The DJ waveform in Figure 7 shows a different contour pattern do than the jerk waveforms. The foveation region shows ripples (due to the high-frequency pendular component), shown in the dotted white ellipse. In pure jerk waveforms (Figs. 1 and 2), these regions are more homogenous.

Figure 8 is another example of inattention in DJ. Power of 12 scale selection was used in this case to show more low-frequency information. The contour plot again clearly showed the two big saccades that brought the eyes back after extended slow phases. The coefficient line of 128 shows the frequency of the jerk component in this DJ waveform. Other coefficient lines would reveal other frequency components.

Wavelet Analysis of INS–Waveform Time Variation

In Figure 9, a highly variable nystagmus over a long fixation period (28 seconds) is presented in the top window. We chose the step-by-step mode with a maximum of 512 steps. The

coefficient line of 28 plotted at the bottom resembles a differentiated version of the signal. As the nystagmus waveform varies, so does the coefficient. In the contour plot, the fast phases are clearly identified in the small (i.e., high-frequency) scales, whereas the inattentive regions where the eyes drift to a halt can be seen at the larger (i.e., low-frequency) scales as relatively static regions of dark shading.

Figure 10 is an example in which the nystagmus is highly variable due to inattention. The segment shown is a concatenated segment of three identical pieces, each piece featuring a bidirectional jerk (solid white ellipse), followed by three cycles of Pfs (dotted white ellipse), a partial blink (solid black ellipse), and total disappearance of the nystagmus (black dash-dot ellipse). The patterns on the contour plot are markedly different in these four parts. Here, the different scales do pick up different waveform features.

DISCUSSION

In addition to eye movements, spectral and wavelet analyses have been widely used in the study of other physiological waveforms such as the electroencephalogram (EEG). The fast Fourier transform (FFT) has been used to examine changes in EEG spectra in diverse applications such as response to differ-
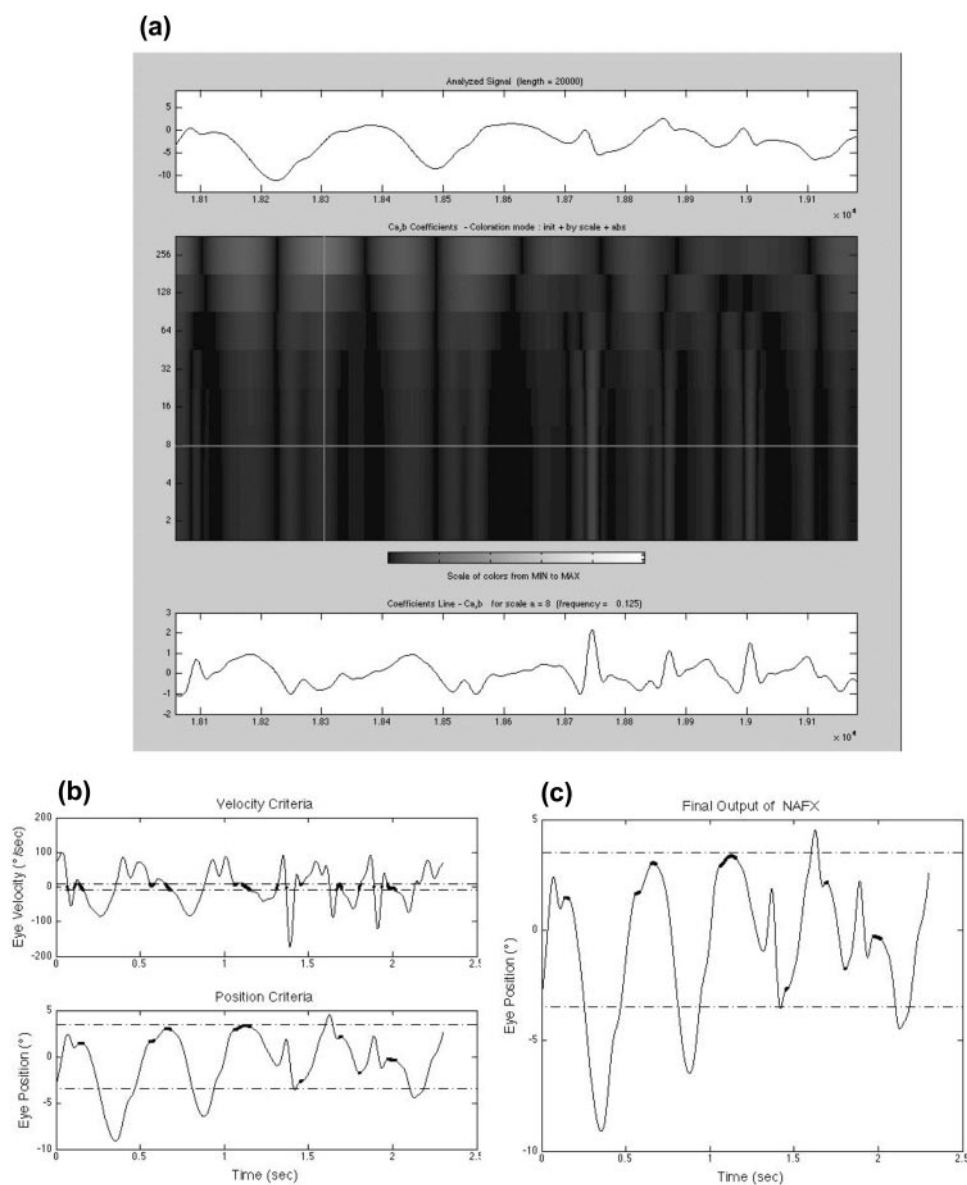
FIGURE 5. (a) One-dimensional continuous wavelet transform of post-tenotomy fixation data from the same patient as in Figure 4 (power 6 in power-2 mode). *Bottom trace:* coefficient line at 8. (b) NAFX analysis of the same data section, the *bold dots* showing the part in the waveform meeting the velocity (*top*) and position (*bottom*) requirement. (c) Output of the NAFX analysis combining the two requirements in (b). The integrated output corresponds to an NAFX value of 0.343, a ~180% increase from the pre-tenotomy value. The *x*-axes are in seconds.

ent odors[43] and the relationship between cardiovascular damage and mild cognitive impairment.[44] The applicability of these techniques is based on a set of assumptions on the statistical properties of the signal being examined. One of them is that the time series being analyzed be stationary (i.e., that its statistical properties not change over time).[45] In ocular motor studies, this assumption makes Fourier analysis well-suited for the study of clearly periodic signals such as smooth pursuit[46] or pendular nystagmus.[47] In such studies, the properties of the entire sample of the waveform are analyzed, with the underlying assumption being that these properties are stable over time. Such techniques are by design insensitive to transient changes in the waveform and can provide no information about the properties of the waveform at a particular instant in time. When transient events have been sought in the EEG, wavelet analysis has been used.[25,26]

One way to identify changes over several seconds is to apply signal analysis techniques over briefer intervals. Short-time Fourier transform analysis (STFT), as pointed out by Hosokawa et al.,[48] showed periodicity in some nystagmus waveforms. The ability to identify time-related changes in the signal, however, is limited by the duration of the windows into which it is divided. The frequency resolution of the STFT also drops as the window becomes briefer.

This study was designed to examine whether wavelet analysis can be successfully applied to study INS. We tried to assess different aspects of INS waveforms: foveation, morphology and time variation. Since conventional spectral analyses are inappropriate when analyzing such nonstationary waveforms, every effort was made to determine whether wavelet analysis, with its ability to represent moment-by-moment changes in signal composition, could enhance our understanding of INS beyond what direct analysis of the waveform itself can show us.

The comparison of waveforms with varying degrees of foveation quality show that wavelet analysis did pick up foveation differences, at least in some simple waveforms. This was achieved by inspecting the "dark areas" after the foveating saccades. How to quantify these areas remains a problem. It may be calculated by integration of the whole area using a signal-processing algorithm. Such a calculation may be possible for jerk waveforms, but would be very difficult for more complicated waveforms like PPfs or mixtures of waveforms.

In the example of the PPfs waveform, without specific knowledge of the significance of each saccade, it is easy to

FIGURE 6. One-dimensional continuous wavelet transform of APAN waveforms (step-by-step mode with a maximum number of 512). *Bottom trace*: the always-present high-frequency pendular component that is sampled with a very low wavelet coefficient. *Solid black ellipse*: several cycles of the left-beating components; *dashed black ellipse*: several cycles of the right-beating ones. The *x*-axes are in milliseconds.
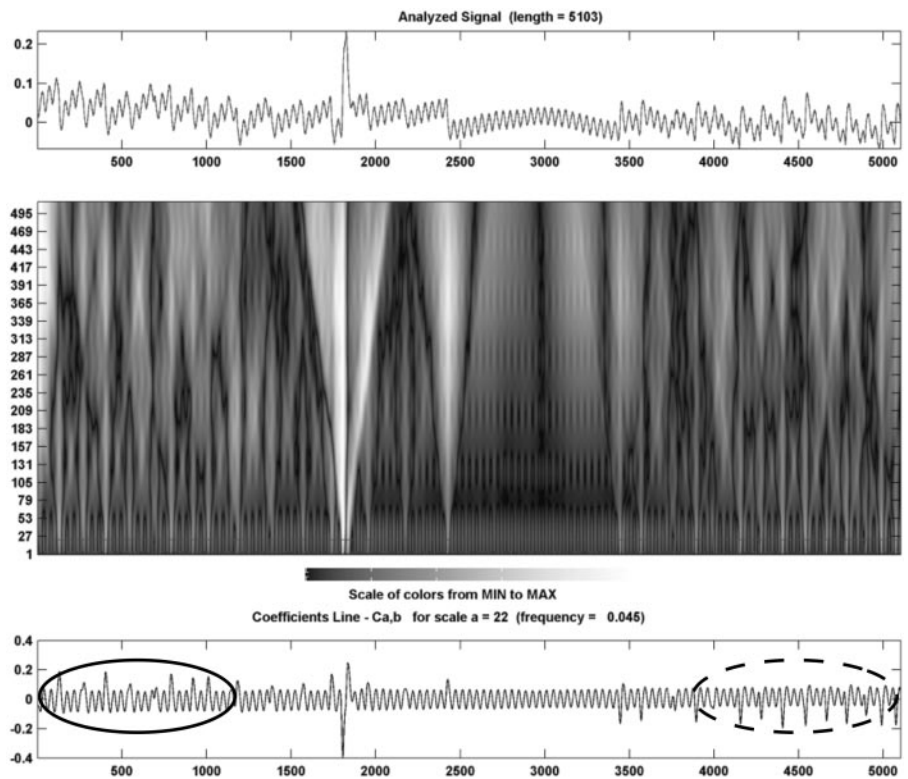

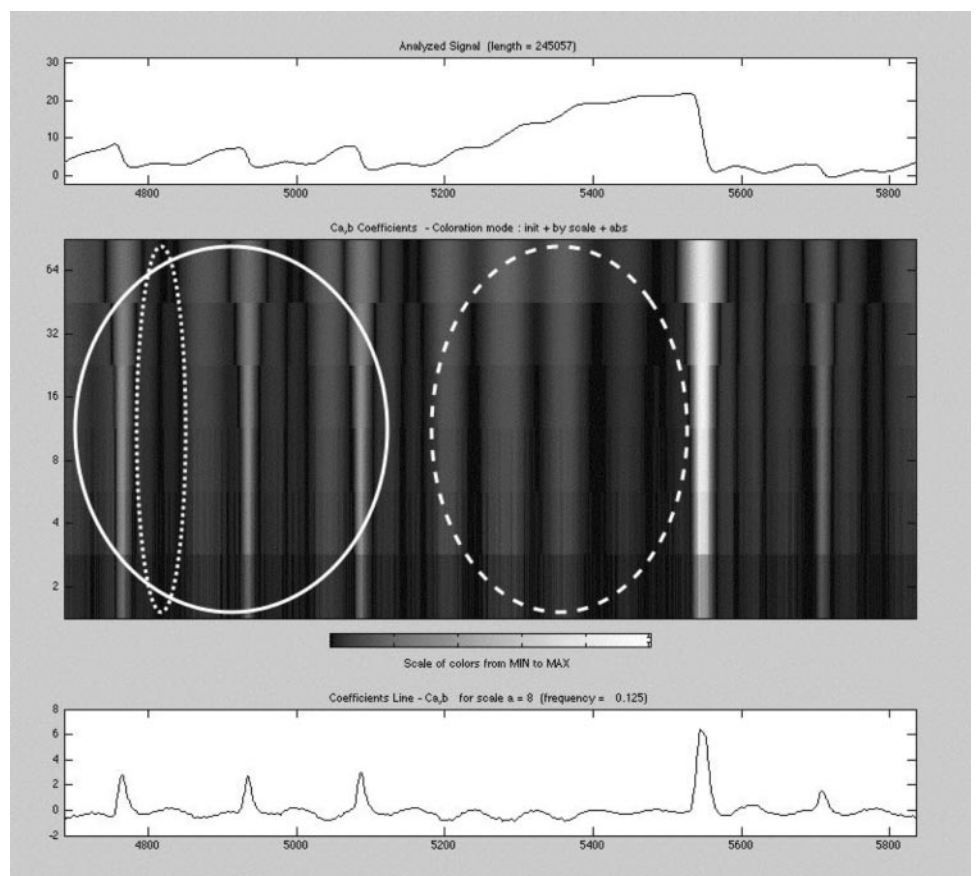**FIGURE 7.** One-dimensional continuous wavelet transform of a data piece containing inattention (power 6 in power-2 mode). *Dotted white ellipse*: an example of target foveation; *dashed white ellipse*: a different pattern than that contained by *solid white ellipse*, because no saccades were made during this inattention period. *Bottom trace*: the coefficient line at 8. The *x*-axes are in milliseconds.
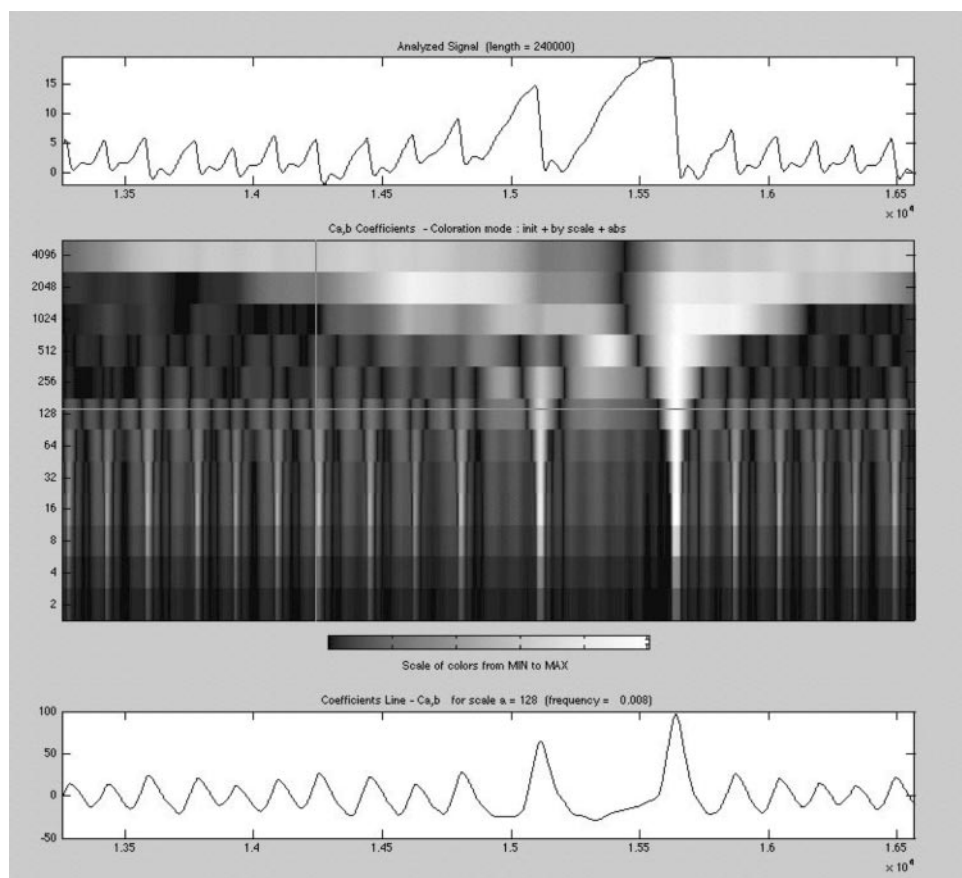
FIGURE 8. One-dimensional continuous wavelet transform of a DJ data piece containing increasing inattention (step-by-step mode with a maximum number of 512). *Bottom trace*: coefficient line at 128. The *x*-axes are in seconds.

confuse the braking saccade with the foveating saccade if one merely examines the contour plot, because both types of saccade terminate a slow eye movement and at least transiently bring the eye to a halt, but only one of them does so when the image of the point of regard is falling on the fovea. Therefore, identification of the foveation periods would also be confused. Visual or computational algorithms are needed to identify the actual foveation period. This screening may be more difficult as

we examine more complicated waveforms and their combinations.

Comparing the pre- and post-tenotomy data, it was difficult to distinguish how foveation changed after the procedure. The actual waveforms are much more variable and complicated than the demonstrations of pure J or pure PPfs (Figs. 1, 2, 3). Therefore, the contour plot had much more variation, making the examination of foveation difficult when using this ap-
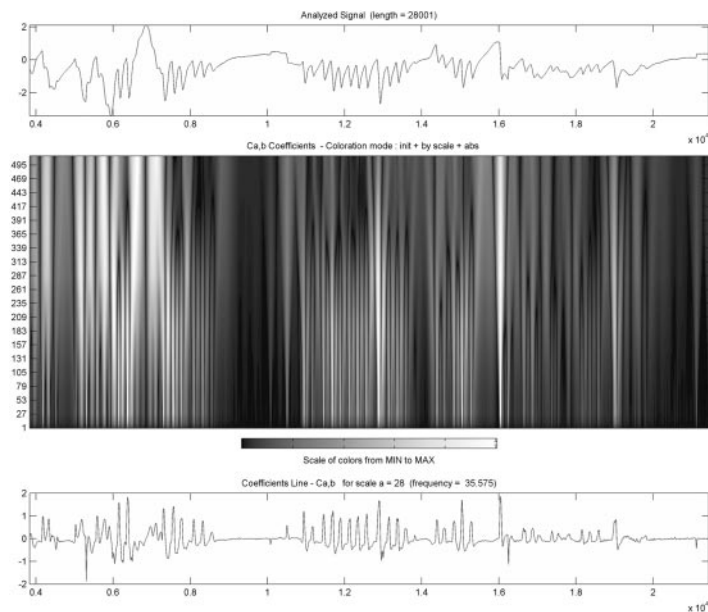

FIGURE 9. One-dimensional continuous wavelet transform of a highly variable nystagmus data section containing intermittent inattention (step-by-step mode with a maximum number of 512). *Bottom trace*: coefficient line at 28. The *x*-axes are in tens of seconds.
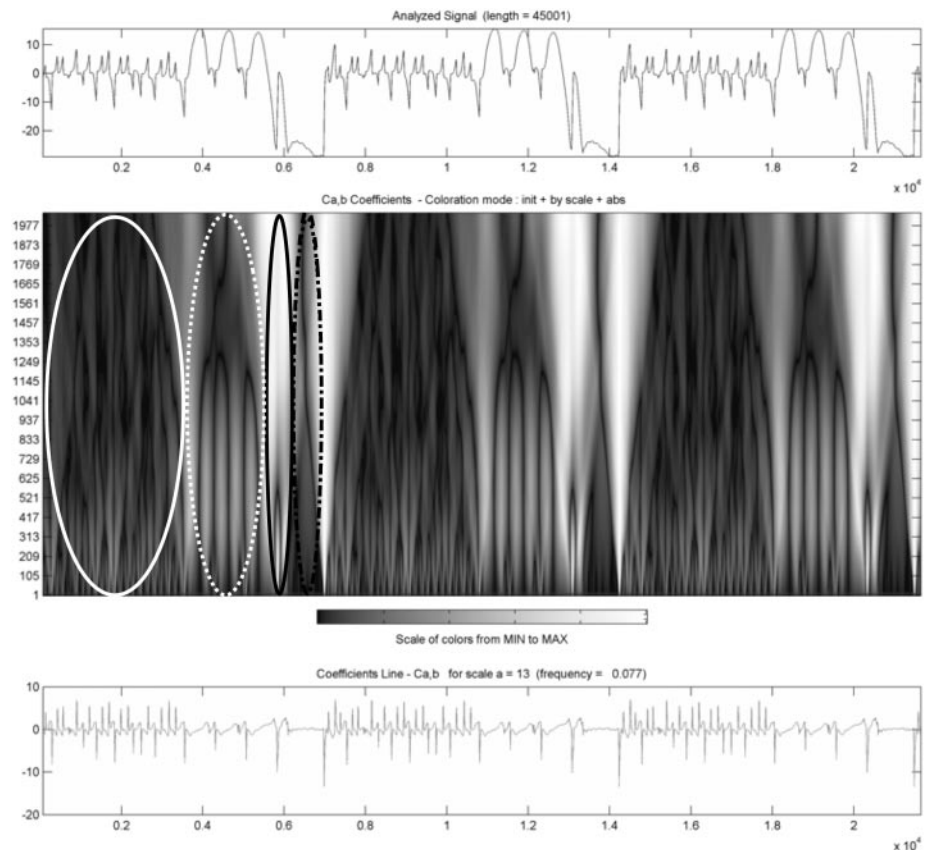
FIGURE 10. One-dimensional continuous wavelet transform of nystagmus data containing inattention and blinking. The segment shown is a concatenated segment of three identical pieces, each piece featuring a bidirectional jerk (*solid white ellipse*), followed by three cycles of Pfs (*dotted white ellipse*), a partial blink (*solid black ellipse*), and total disappearance of the nystagmus (*black dash-dot ellipse*). *Bottom trace*: a very low wavelet coefficient. The x-axes are in tens of seconds.

proach. The NAFX specifically analyzes the foveation periods in a position and velocity window (eliminating all other portions of the waveform), and therefore gives a quantitative and objective number identifying the foveation quality.[9]

Wavelet analysis is a complex and computationally intensive method for the task of examining foveation quality, something that can be done much more simply and accurately by using the NAFX. Because best visual acuity depends on the target image's being on or near the fovea and moving at minimal velocity,[2,9,12,28,49,50] it appears that a more direct operation on the eye position time series itself gives the needed information more simply than does wavelet analysis. Wavelet analysis may be of some use in examining the morphologic characteristics of INS waveforms. The low-span (high-frequency) coefficients could be used as fast-phase detectors, although it remains to be seen if this is more efficient than simple differentiation of the initial waveform. An application that takes advantage of the ability of wavelet analysis to represent waveform morphology may be to use a fixed number of coefficients to identify waveforms automatically as they change in a given record, perhaps by training a neural network to recognize exemplars of each waveform. Although such waveforms are easy for experienced observers to identify by visual inspection, such a process may make identification available more widely. It may also be useful in attempting to quantify how much time is spent in various waveforms or how they change under experimental or clinical manipulation. Similarly, it may be possible to use it to quantify how APAN components and fast-phase directions change across time. Wavelet analysis could be combined with electrophysiological measures of arousal or stress, to provide quantitative, moment-by-moment information about how these changes in internal state affect the INS waveform. Averaging the coefficients in wavelet analysis of INS, as in Miura et al.,[30] unfortunately obscures the key

advantage of wavelet analysis— capturing temporal variations in waveform morphology. This averaging essentially treats the waveform as stationary and renders the wavelet analysis equivalent to Fourier analysis. It thus would have been unable to distinguish any morphologic or foveation characteristics of INS waveforms.

The nonstationary nature of INS also raises the question of which data from a recording session should be analyzed. One approach, familiar to engineers, is to apply some form of time series analysis to the entire record. This approach assumes that the results of some experimental manipulation or clinical intervention, to be significant, must affect the major components of the signal. An example of this was the comparison by Roberti et al.[51] of spectral analysis and intensity calculation in evaluating several surgical approaches to treating INS. Their justification for the "whole of signal" approach can be found in their statement, "We regarded each signal recording as a realization of a stochastic process, supposed stationary at least to the second moment. In fact, different samples of signal recorded at different times, for the same patient and angular position, resemble each other only in their average properties, owing to the presence of noise and small random changes in the nystagmus waveform pattern."[51] They identified the peak of the power spectrum and used its amplitude and frequency, as well as evaluation of the power plot, to characterize the effects of nystagmus surgery. Similarly, Miura et al.[30] operated on the entire recorded datasets, averaging the log ratio of the wavelet spectra in a 4- to 10-minute "fixation" recording. There are several problems with doing this when evaluating the effects of an intervention. First, as noted by Roberti et al.,[51] is the unavoidable presence of noise in the recording, both intrinsic to the recording system and arising from blinks, facial motion, and the like. Furthermore, by operating on the entire recording, the effects on the signal of changes in the fixating

eye (in strabismic patients), of losses of fixation and of lapses in attention are not separated out. When a task consists of gazing at a target for minutes on end, these are all common, real influences on the nature of the nystagmus waveform. Blinks and inattention, shown in Figures 7, 8, and 10, are also frequently present in INS data. These contaminants of the signal are extremely likely to affect the outcome of any sort of global analysis far more than would an increase in the duration of foveation periods, which constitute in many patients only a small percentage of the total signal. Thus, averaging segments containing these artifacts would include data with no functional (foveation) importance.

It is, therefore, more appropriate to analyze only those relatively brief segments of data taken around the time a target has been fixated and to do so in a way that explicitly quantifies the quality of foveation, which is the visually important characteristic of the INS waveform. For this reason, the durations of recording samples used to quantify nystagmus characteristics have ranged from 3 to 20 seconds.[7,8,13,14,52–54] The NAFX analysis,[9] used in several studies,[10,20,21,40,41,55,56] inspects each fixation segment to determine the foveation quality in that segment; several NAFX values are averaged to reflect the subject's ability to fixate. Any blink or inattention data are excluded from the NAFX analysis. Therefore, NAFX is a much more direct and objective methodology to perform INS analysis, especially one that correlates with visual acuity. The use of wavelets does not appear to be sensitive enough for all waveforms to detect the changes in foveation quality brought about by current therapies.

To summarize, wavelet analyses shows some sensitivity to different features of the waveform and reflects variations across time. Indeed, it is very sensitive to the latter. It may have a role in developing automated waveform classifiers or in other applications in which its time-dependent characterization of the waveform can be put to best use. In the examination of foveation, the visually most important feature of the INS waveform, wavelet analysis is a tool that performs, with difficulty, some things that can be done faster and better by directly operating on the nystagmus waveform itself. It appears, however, to be insensitive to the subtle but visually important improvements brought about by INS therapies.

References

1. CEMAS_Working_Group. *A National Eye Institute Sponsored Workshop and Publication on The Classification of Eye Movement Abnormalities and Strabismus* (CEMAS). Bethesda, MD: National Institutes of Health, National Eye Institute; 2001. Available at www.nei.nih.gov.

2. Abadi RV, Bjerre A. Motor and sensory characteristics of infantile nystagmus. *Br J Ophthalmol*. 2002;86:1152–1160.

3. Dell'Osso LF. Congenital, latent and manifest latent nystagmus: similarities, differences and relation to strabismus. *Jpn J Ophthalmol*. 1985;29:351–368.

4. Hertle RW, Maldanado VK, Maybodi M, Yang D. Clinical and ocular motor analysis of the infantile nystagmus syndrome in the first 6 months of life. *Br J Ophthalmol*. 2002;86:670–675.

5. Cham KM, Anderson AJ, Abel LA. Task-induced stress and motivation decrease foveation-period durations in infantile nystagmus syndrome. *Invest Ophthalmol Vis Sci*. Published online April 17, 2008.

6. Dell'Osso LF, Daroff RB. Congenital nystagmus waveforms and foveation strategy. *Doc Ophthalmol*. 1975;39:155–182.

7. Abadi RV, Worfolk R. Retinal slip velocities in congenital nystagmus. *Vision Res*. 1989;29:195–205.

8. Zubcov AA, Stark N, Weber A, Wizov SS, Reinecke RD. Improvement of visual acuity after surgery for nystagmus. *Ophthalmology*. 1993;100:1488–1497.

9. Dell'Osso LF, Jacobs JB. An expanded nystagmus acuity function: intra- and intersubject prediction of best-corrected visual acuity. *Doc Ophthalmol*. 2002;104:249–276.

10. Hertle RW, Dell'Osso LF, FitzGibbon EJ, Yang D, Mellow SD. Horizontal rectus muscle tenotomy in patients with infantile nystagmus syndrome: a pilot study. *J AAPOS*. 2004;8:539–548.

11. Yang D, Hertle RW, Hill VM, Stevens DJ. Gaze-dependent and time-restricted visual acuity measures in patients with infantile nystagmus syndrome (INS). *Am J Ophthalmol*. 2005;139:716–718.

12. Abadi RV, Dickinson CM. Waveform characteristics in congenital nystagmus. *Doc Ophthalmol*. 1986;64:153–167.

13. Abel LA, Williams IM, Levi L. Intermittent oscillopsia in a case of congenital nystagmus: dependence upon waveform. *Invest Ophthalmol Vis Sci*. 1991;32:3104–3108.

14. Bedell HE, White JM, Abplanalp PL. Variability of foveations in congenital nystagmus. *Clin Vis Sci*. 1989;4:247–252.

15. Dell'Osso LF, Leigh RJ. Foveation period stability and oscillopsia suppression in congenital nystagmus. *Neuro-ophthalmol*. 1992;12:169–183.

16. Dell'Osso LF, Leigh RJ. Ocular motor stability of foveation periods: Required conditions for suppression of oscillopsia. *Neuro-ophthalmol*. 1992;12:303–326.

17. Leigh RJ, Dell'Osso LF, Yaniglos SS, Thurston SE. Oscillopsia, retinal image stabilization and congenital nystagmus. *Invest Ophthalmol Vis Sci*. 1988;29:279–282.

18. Mezawa M, Ishikawa S, Ukai K. Changes in waveform of congenital nystagmus associated with biofeedback treatment. *Br J Ophthalmol*. 1990;74:472–476.

19. Tkalcevic L, Abel LA. The effects of increased visual task demand on foveation in congenital nystagmus. *Vision Res*. 2005;45:1139–1146.

20. Hertle RW, Dell'Osso LF, FitzGibbon EJ, Thompson D, Yang D, Mellow SD. Horizontal rectus tenotomy in patients with congenital nystagmus: results in 10 adults. *Ophthalmology*. 2003;110:2097–2105.

21. Wang Z, Dell'Osso LF, Jacobs JB, Burnstine RA, Tomsak RL. Effects of tenotomy on patients with infantile nystagmus syndrome: foveation improvement over a broadened visual field. *J AAPOS*. 2006;10:552–560.

22. Augustyniak P. *Advanced method of nystagmus-phase separation using adaptive modification of time-frequency signal representation.* Third International Conference on Signal Processing. Beijing, China: IEEE; 1996:351–354.

23. Mahmoodabadi SZ, Ahmadian A, Abolhasani MD, Eslami M, Bidgoli JH. *ECG feature extraction based on multiresolution wavelet transform.* Twenty-seventh Annual Conference of the IEEE Engineering in Medicine and Biology Society. Shanghai, China: IEEE; 2005:3902–3905.

24. Pope MH, Aleksiev A, Panagiotacopulos ND, et al. Evaluation of low back muscle surface EMG signals using wavelets. *Clin Biomechan*. 2000;15:567–573.

25. Muthuswamy J, Thakor NV. Spectral analysis methods for neurological signals. *J Neurosci Methods*. 1998;83:1–4.

26. Sajda P, Laine A, Zeevi Y. Multi-resolution and wavelet representations for identifying signatures of disease. *Dis Markers*. 2002;18:339–363.

27. Dell'Osso LF. Functional definitions and classification of congenital nystagmus waveforms. *Ophthalmol Digest*. 1976;38:19–27.

28. Dell'Osso LF. Congenital nystagmus waveforms and foveation strategy (in German). In: Kommerell G, ed. *Augenbewegungsstorungen, Neurophysiologie und Klinik Symposion der Deutschen Ophthalmologischen Gesellschaft*. München: Bergmann-Verlag; 1978:353–356.

29. Miura K, Hertle RW, FitzGibbon EJ, Optican LM. Effects of tenotomy surgery on congenital nystagmus waveforms in adult patients. Part II. Dynamical systems analysis. *Vision Res*. 2003;43:2357–2362.

30. Miura K, Hertle RW, FitzGibbon EJ, Optican LM. Effects of tenotomy surgery on congenital nystagmus waveforms in adult patients. Part I. Wavelet spectral analysis. *Vision Res*. 2003;43:2345–2356.

31. Anderson JR. Causes and treatment of congenital eccentric nystagmus. *Br J Ophthalmol*. 1953;37:267–281.

32. Kestenbaum A. Nouvelle operation de nystagmus. *Bull Soc Ophthalmol Fr.* 1953;6:599–602.

33. Kestenbaum A. *A nystagmus operation.* Acta XVII Council on Ophthalmology (Canada, United States). 1954;ii:1071–1078.

34. Dell'Osso LF, Flynn JT. Congenital nystagmus surgery: a quantitative evaluation of the effects. *Arch Ophthalmol.* 1979;97:462–469.

35. Dell'Osso LF. Extraocular muscle tenotomy, dissection, and suture: a hypothetical therapy for congenital nystagmus. *J Pediatr Ophthalmol Strabismus.* 1998;35:232–233.

36. Dell'Osso LF, Hertle RW, Williams RW, Jacobs JB. A new surgery for congenital nystagmus: effects of tenotomy on an achiasmatic canine and the role of extraocular proprioception. *J AAPOS.* 1999; 3:166–182.

37. Wang Z, Dell'Osso LF, Zhang Z, Leigh RJ, Jacobs JB. Tenotomy does not affect saccadic velocities: support for the "small-signal" gain hypothesis. *Vision Res.* 2006;46:2259–2267.

38. Hertle RW, Dell'Osso LF. Clinical and ocular motor analysis of congenital nystagmus in infancy. *J AAPOS.* 1999;3:70–79.

39. Hertle RW, Dell'Osso LF, FitzGibbon EJ, Thompson D, Yang D. Mellow SD. *Protocol 99-EI-0152: horizontal rectus tenotomy in the treatment of congenital nystagmus.* Bethesda, MD: The National Eye Institute, National Institutes of Health, Intramural Research Protocols; 1999;1–85.

40. Tomsak RL, Dell'Osso LF, Rucker JC, Leigh RJ, Bienfang DC, Jacobs JB. Treatment of acquired pendular nystagmus from multiple sclerosis with eye muscle surgery followed by oral memantine. DJO (*Digital Journal of Ophthalmology*). 2005;11:1–11.

41. Wang ZI, Dell'Osso LF, Tomsak RL, Jacobs JB. Combining recessions (nystagmus and strabismus) with tenotomy improved visual function and decreased oscillopsia and diplopia in acquired downbeat nystagmus and in horizontal infantile nystagmus syndrome. *J AAPOS.* 2007;11:135–141.

42. Misiti M, Misiti Y, Oppenheim G, Poggi J-M. *Wavelet Toolbox for Use with MatLab.* 2nd ed. Natick, MA: The MathWorks, Inc.; 2000.

43. Murali S, Vladimir KS. Analysis of fractal and fast Fourier transform spectra of human electroencephalograms induced by odors. *Int J Neurosci.* 2007;117:1383–1401.

44. Moretti DV, Miniussi C, Frisoni G, et al. Vascular damage and EEG markers in subjects with mild cognitive impairment. *Clin Neurophysiol.* 2007;118:1866–1876.

45. Donnelly D. The fast Fourier transform for experimentalists, Part VI: Chirp of a bat. *Comput Sci Eng.* 2006;8:72–78.

46. Baloh RW, Langhofer L, Honrubia V, Yee RD. On-line analysis of eye movements using a digital computer. *Aviat Space Environ Med.* 1980;51:563–567.

47. Reccia R, Roberti G, Russo P. Spectral analysis of pendular waveforms in congenital nystagmus. *Ophthalmic Res.* 1989;21:83–92.

48. Hosokawa M, Hasebe S, Ohtsuki H, Tsuchida Y. Time-frequency analysis of electronystagmogram signals in patients with congenital nystagmus. *Jpn J Ophthalmol.* 2004;48:262–267.

49. Bedell HE, Loshin DS. Interrelations between measures of visual acuity and parameters of eye movement in congenital nystagmus. *Invest Ophthalmol Vis Sci.* 1991;32:416–421.

50. Dell'Osso LF, Leigh RJ, Sheth NV, Daroff RB. Two types of foveation strategy in 'latent' nystagmus: fixation, visual acuity and stability. *Neuro-ophthalmology.* 1995;15:167–186.

51. Roberti G, Russo P, Segr G. Spectral analysis of electro-oculograms in the quantitative evaluation of nystagmus surgery. *Med Biol Eng Comp.* 1987;25:573–576.

52. Bosone G, Reccia R, Roberti G, Russo P. Frequency distribution of the time interval between quick phase nystagmic eye movements. *Ophthalmic Res.* 1990;22:178–182.

53. Dell'Osso LF, Van der Steen J, Steinman RM, Collewijn H. Foveation dynamics in congenital nystagmus. I. Fixation. *Doc Ophthalmol.* 1992;79:1–23.

54. Hanson KS, Bedell HE, White JM, Ukwade MT. Distance and near visual acuity in infantile nystagmus. *Optom Vis Sci.* 2006;83:823–829.

55. Jacobs JB, Dell'Osso LF, Hertle RW, Acland GM, Bennett J. Eye movement recordings as an effectiveness indicator of gene therapy in RPE65-deficient canines: implications for the ocular motor system. *Invest Ophthalmol Vis Sci.* 2006;47:2865–2875.

56. Sarvananthan N, Proudlock FA, Choudhuri I, Dua H, Gottlob I. Pharmacologic treatment of congenital nystagmus. *Arch Ophthalmol.* 2006;124:916–918.